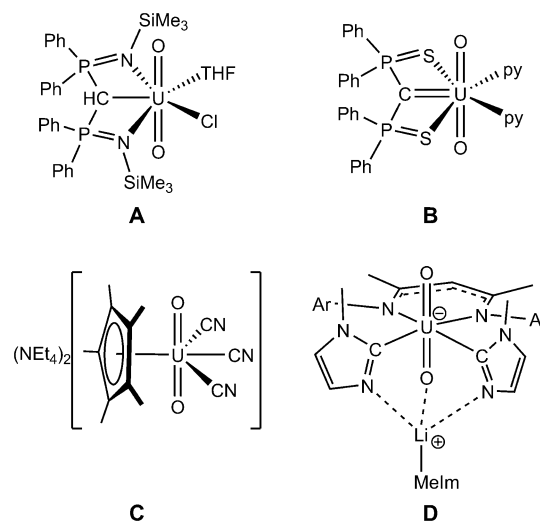


# A Rare Uranyl(VI)–Alkyl Ate Complex $[\text{Li}(\text{DME})_{1.5}]_2[\text{UO}_2(\text{CH}_2\text{SiMe}_3)_4]$ and Its Comparison with a Homoleptic Uranium(VI)–Hexaalkyl\*\*

Lani A. Seaman, Peter Hrobárik,\* Michael F. Schettini, Skye Fortier, Martin Kaupp, and Trevor W. Hayton\*

Beginning with the Manhattan Project,<sup>[1]</sup> uranium–alkyl complexes have been a coveted target in the actinide chemistry. The initial interest in these complexes was due to their anticipated volatility, which would permit their use in gas-phase isotope separation.<sup>[1–3]</sup> In the 70 years since the Manhattan Project, the organometallic chemistry of uranium has flourished,<sup>[2]</sup> however, this chemistry has been dominated by the 3+ and 4+ oxidation states. In contrast, the organometallic chemistry of the 5+ and 6+ states has lagged behind considerably.<sup>[4–6]</sup> This is especially true for the uranyl ion, the most studied fragment in uranium chemistry.<sup>[7]</sup> Despite the fact that the preparation of organometallic uranyl complexes has been attempted for over 150 years,<sup>[8]</sup> the first uranyl–hydrocarbyl complex was only reported in 2002.<sup>[9]</sup> It is now clear that many initial synthetic attempts resulted only in uranyl reduction, and not in alkylation.<sup>[10]</sup> For example, Ephritikhine and co-workers demonstrated that reaction of one equivalent of  $\text{Li}(\text{CH}_2\text{SiMe}_3)$  with  $[\text{UO}_2\text{I}_2(\text{THF})_3]$  or  $[\text{UO}_2(\text{OTf})_2]$  in pyridine resulted in the formation of a uranyl(V) complex,<sup>[11]</sup> while Seyam observed formation of  $\text{UO}_2$  and biphenyl upon reaction of  $\text{UO}_2\text{Cl}_2$  with two equivalents of phenyllithium.<sup>[12]</sup>

Only recently have chemists developed strategies for inhibiting the reduction of uranyl. For example, Sarsfield et al. used a chelating bis(iminophosphorano) ligand to stabilize the U–C bond in  $[(\text{BIPMH})\text{UO}_2\text{Cl}(\text{THF})]$  (**A**, BIPMH =



**Scheme 1.** Schematic structure of the recently synthesized uranyl complexes with direct U–C  $\sigma$  bonds. MeIm = 1-methylimidazole, py = pyridine.

$\text{HC}(\text{PPh}_2\text{NSiMe}_3)_2$ ; Scheme 1).<sup>[9,13]</sup> This strategy was later employed in the synthesis of the first uranyl–methanediide complex,  $[\text{UO}_2(\text{SCS})(\text{py})_2]$  (**B**,  $\text{SCS}^{2-} = [\text{C}(\text{Ph}_2\text{PS})_2]^{2-}$ ).<sup>[14]</sup> Also notable is the synthesis of the first cyclopentadienyl complex of uranyl,  $[\text{NEt}_4]_2[(\text{C}_5\text{Me}_5\text{UO}_2(\text{CN})_3)]$  (**C**),<sup>[15]</sup> formed by oxygen atom transfer to a  $\text{U}^{\text{IV}}$ –cyclopentadienyl precursor. Finally, our research group demonstrated that uranyl–carbon  $\sigma$  bonds could be stabilized by steric saturation of the uranium coordination sphere (so-called “ate” complex formation), as in the case of the bis(imidazolyl) complex,  $[\text{Li}(\text{MeIm})][\text{UO}_2(\text{Ar}_2\text{nacnac})(\text{C}_4\text{H}_5\text{N}_2)_2]$  (**D**),<sup>[16]</sup> which exhibits unusual thermal stability for a  $\text{U}^{\text{VI}}$ –hydrocarbyl complex.

The strategy of “ate” complex formation has also allowed us to stabilize several homoleptic uranium–alkyl complexes in the 4+, 5+, and 6+ oxidation states, as well as several homoleptic thorium–alkyl complexes.<sup>[5,17,18]</sup> Their synthesis and characterization, in conjunction with quantum-chemical calculations, has enabled the study of the contribution of the 6d and 5f valence orbitals in actinide–carbon bonds. These results inspired us to explore the synthesis of a uranyl–alkyl “ate” complex to gain further insight into the U–C bonding interactions. Herein, we describe the synthesis of the rare uranyl(VI)–alkyl complex  $[\text{Li}(\text{DME})_{1.5}]_2[\text{UO}_2(\text{CH}_2\text{SiMe}_3)_4]$  (**1**) and an analysis of its electronic structure by relativistic

[\*] Dr. L. A. Seaman, M. F. Schettini, Dr. S. Fortier, Prof. Dr. T. W. Hayton  
Department of Chemistry and Biochemistry  
University of California Santa Barbara  
Santa Barbara, CA 93106 (USA)  
E-mail: hayton@chem.ucsb.edu

Dr. P. Hrobárik, Prof. Dr. M. Kaupp  
Institut für Chemie, Technische Universität Berlin  
Strasse des 17. Juni 135, 10623 Berlin (Germany)  
E-mail: peter.hrobarik@savba.sk

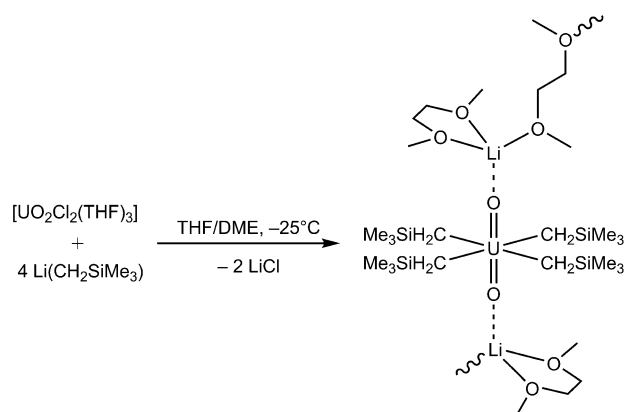
Dr. P. Hrobárik  
Institute of Inorganic Chemistry, Slovak Academy of Sciences  
Dúbravská cesta 9, 84536 Bratislava (Slovakia)

[\*\*] This work was supported by the U.S. Department of Energy, Office of Basic Energy Sciences, Chemical Sciences, Biosciences and Geosciences Division (Contract No. DE-FG02-09ER16067) and by the Berlin DFG cluster of excellence on “Unifying Concepts in Catalysis” (UniCat). We also thank Dr. Guang Wu for assistance with the X-ray crystallographic determination. P.H. gratefully acknowledges the Alexander von Humboldt foundation for a research fellowship.

Supporting information for this article is available on the WWW under <http://dx.doi.org/10.1002/anie.201209611>.

DFT calculations for comparison with a homoleptic hexaalkyl-uranium(VI) complex,  $[\text{U}(\text{CH}_2\text{SiMe}_3)_6]$  (**2**). Furthermore, the revised  $^{13}\text{C}$  NMR spectrum of **2** is presented, and the origin of the unprecedentedly downfield methylene  $^{13}\text{C}$  NMR chemical shifts in **1** and **2** is analyzed and put in contrast with those of the analogous  $\text{W}^{\text{VI}}$  and  $\text{Th}^{\text{IV}}$  complexes.

Addition of a cold ( $-25^\circ\text{C}$ ) solution of  $[\text{UO}_2\text{Cl}_2(\text{THF})_3]$  in THF to a cold ( $-25^\circ\text{C}$ ) solution of  $\text{Li}(\text{CH}_2\text{SiMe}_3)$  (4 equiv) in 1,2-dimethoxyethane (DME) results in an immediate color change to red. Rapid removal of the volatiles and extraction into hexanes gives a green-brown solution. Storage at  $-25^\circ\text{C}$  for 12 hours results in the precipitation of the uranyl-alkyl complex  $[\text{Li}(\text{DME})_{1.5}]_2[\text{UO}_2(\text{CH}_2\text{SiMe}_3)_4]$  (**1**) as a green crystalline solid in 24% yield (see Scheme 2). Complex **1** is soluble in hexanes, ethereal solvents, and aromatic solvents, but decomposes in  $\text{CH}_2\text{Cl}_2$ . Additionally, complex **1** is temperature-sensitive, decomposing completely over two hours at room temperature in  $[\text{D}_8]\text{THF}$ , according to NMR spectroscopy. The  $^1\text{H}$  NMR spectrum of **1** at  $-1.6^\circ\text{C}$  in  $[\text{D}_8]\text{THF}$  exhibits resonances at 0.01 and  $-3.80$  ppm, corresponding to the methyl and methylene groups, respectively. The  $^7\text{Li}$  NMR spectrum in  $\text{C}_6\text{D}_6$  at room temperature exhibits a single resonance at 2.93 ppm, consistent with a single lithium environment. Finally, the  $^{13}\text{C}\{^1\text{H}\}$  NMR spectrum in  $[\text{D}_8]\text{THF}$  exhibits a resonance at 10.6 ppm, which can be attributed to the methyl groups of the methyltrimethylsilyl ligand. More notably, the methylene resonance of the  $\text{CH}_2\text{SiMe}_3$  ligand is significantly deshielded at 242.9 ppm (see Table 1 for the corresponding  $^{13}\text{C}$  NMR shifts in  $\text{WO}_2^{2+}$  analogues). This observation coincides with the recent finding that the chemical shifts of nuclei that are  $\sigma$ -bonded to the  $f^0$  actinide center can be shifted to extremely high frequency because of relativistic spin-orbit (SO) effects (see also below).<sup>[19,20]</sup> The observed  $^{13}\text{C}$  NMR chemical shift also provides strong evidence for the presence of Li–O(uranyl) interactions in solution (see below).



**Scheme 2.** Synthesis of  $[\text{Li}(\text{DME})_{1.5}]_2[\text{UO}_2(\text{CH}_2\text{SiMe}_3)_4]$  (**1**).

Complex **1** crystallizes in the triclinic space group  $P\bar{1}$  and its solid-state molecular structure is shown in Figure 1.<sup>[21]</sup> The uranium atom in **1** is located on a crystallographically imposed inversion center and is found in a nearly octahedral geometry ( $\text{C1-U1-C5}$   $87.3(2)^\circ$ ,  $\text{C1-U1-C5}^*$   $92.7(2)^\circ$ ,  $\text{C1-U1-C1}^*$   $180^\circ$ ,  $\text{C5-U1-C5}^*$   $180^\circ$ ), coordinated by the two oxygen atoms of the uranyl fragment and the four carbon atoms of the methyltrimethylsilyl ligands. The O–U–O angle in **1** ( $\text{O1-U1-O1}^*$   $180^\circ$ ) is typical of the uranyl fragment; however, the U–O bond length ( $\text{U1-O1}$   $1.885(4)$  Å) is substantially longer than characteristic uranyl(VI) U–O distances ( $1.76$ – $1.79$  Å).<sup>[22,23]</sup> Our computations show that this elongation is due to coordination of the  $\text{Li}^+$  counterions to the uranyl oxo ligands (Table 1). This Lewis-type interaction also leads to a substantially smaller U–C bond length (by  $0.08$  Å) when compared to the naked  $[\text{UO}_2(\text{CH}_2\text{SiMe}_3)_4]^{2-}$  anion.

The U–C bond lengths in **1** ( $\text{U1-C1}$   $2.497(6)$  Å,  $\text{U1-C5}$   $2.481(6)$  Å) are similar to those of other  $\sigma$ -bonded uranium–hydrocarbyl complexes. For example, the U–C bond lengths

**Table 1:** Selected mean bond lengths, NLMO hybridization analysis of the M–C  $\sigma$  bonds and  $^{13}\text{C}$  NMR shifts (in ppm versus TMS) of the metal-bound carbon atoms in  $[\text{UO}_2\text{R}_4]^{2-}$ ,  $[\text{UR}_6]$ ,  $[\text{ThR}_5]$  ( $\text{R} = \text{CH}_3$ ,  $\text{CH}_2\text{SiMe}_3$ ) and their  $\text{W}^{\text{VI}}$  analogues<sup>[a,b]</sup>

Complex	$d(\text{M}-\text{O})$ [Å]	$d(\text{M}-\text{C})$ [Å]	NPA charges $q(\text{M})$ $q(\text{C})$	NLMO analysis of M–C $\sigma$ bonds %M s p d f	$\delta(\text{SR})$ [ppm]	$\delta(\text{SO})$ [ppm]	$\delta(\text{total})$ [ppm]	$\delta(\text{expt.})$ [ppm]
$[\text{UO}_2(\text{CH}_3)_4]^{2-}$	1.806	2.574	1.767 $-1.108$	19.3 17.5 0.2 38.1 44.2	13.2	116.4	129.6	
$[\text{UO}_2(\text{CH}_2\text{SiMe}_3)_4]^{2-}$	1.795	2.573	1.744 $-1.344$	18.0 15.6 0.1 39.5 44.7	37.7	78.5	116.2	
$[\text{Li}(\text{DME})_{1.5}]_2[\text{UO}_2(\text{CH}_2\text{SiMe}_3)_4]$	1.857	2.493	1.670 $-1.296$	21.9 12.7 0.0 34.1 53.2	73.7	177.1	250.8	242.9 <sup>[c]</sup>
<i>cis</i> - $[\text{WO}_2(\text{CH}_2\text{SiMe}_3)_4]^{2-}$	1.758	2.360	1.943 $-1.340$	18.3 16.1 0.2 83.6 0.1	16.1	1.4	17.5	(19.2 <sup>[d]</sup> )
<i>trans</i> - $[\text{WO}_2(\text{CH}_2\text{SiMe}_3)_4]^{2-}$	1.787	2.311	1.825 $-1.258$	23.9 14.1 0.1 85.7 0.1	30.3	8.7	39.0	
$[\text{U}(\text{CH}_3)_6]$		2.343	1.724 $-1.025$	28.6 9.7 0.1 22.6 67.6	125.4	368.1	493.5	
$[\text{U}(\text{CH}_2\text{SiMe}_3)_6]$		2.335	1.309 $-1.221$	28.9 7.2 0.1 24.8 67.9	181.2	347.9	529.1	434.3 <sup>[c]</sup>
$[\text{Th}(\text{CH}_2\text{SiMe}_3)_5]^+$		2.540	2.072 $-1.482$	13.2 18.4 0.4 64.7 16.5	43.7	35.6	79.3	83.0 <sup>[e]</sup>
$[\text{W}(\text{CH}_3)_6]$		2.165	1.674 $-0.951$	32.8 11.8 0.1 88.0 0.1	62.6	20.4	83.0	83.6 <sup>[f]</sup>
$[\text{W}(\text{CH}_2\text{SiMe}_3)_6]$		2.182	1.728 $-1.229$	30.6 10.1 0.1 89.8 0.0	78.0	20.9	98.8	

[a] Optimization and NPA/NLMO analysis done at the PBE0/TZVP level using a small-core quasirelativistic ECPs for the metal centers.

[b] Calculations of NMR shifts performed at the 2c-ZORA-SO level using PBE0-40HF hybrid functional and TZ2P all-electron basis set (see Computational Details in the Supporting Information for more details).  $\delta_{\text{SR}}$  stands for NMR shifts calculated using scalar relativistic effects only, and  $\delta_{\text{SO}}$  for the spin-orbit contribution.

[c] This work. See also the Supporting Information for more details. [d]  $^{13}\text{C}$  NMR shift of methylene group reported for  $[\text{WO}_2(\text{Cp})(\text{CH}_2\text{SiMe}_3)]$ , see Ref. [27]. [e] See Ref. [18]. [f] See Ref. [28].

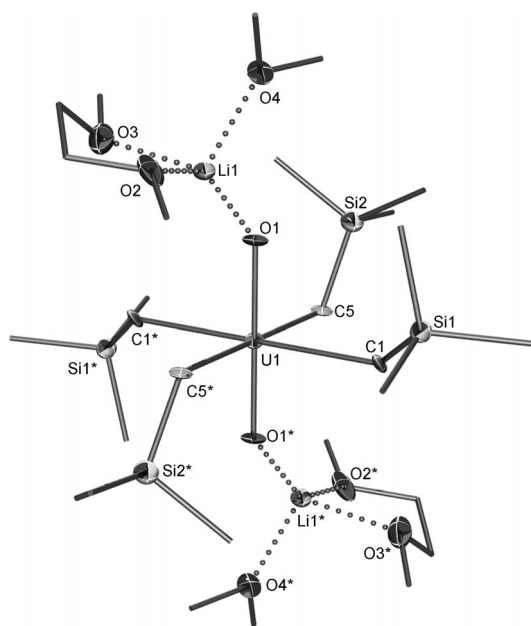


**Figure 1.** ORTEP diagram of  $[\text{Li}(\text{DME})_{1.5}]_2[\text{U}(\mu\text{-O})_2(\text{CH}_2\text{SiMe}_3)_4]$  (**1**) with 50% probability ellipsoids. Selected bond lengths [Å] and angles [°]: U1–O1 1.885(4), U1–C1 2.497(6), U1–C5 2.481(6), Li1–O1 1.87(1), Li1–O2 2.02(1), Li1–O3 2.00(1), Li1–O4 1.98(1), O1–U1–O1\* 180, C1–U1–C5 87.3(2), C1–U1–C5\* 92.7(2), C1–U1–C1\* 180, C5–U1–C5\* 180, O1–Li1–O2 136.5(6), O1–Li1–O3 117.0(7), O1–Li1–O4 113.7(6), O2–Li1–O3 83.2(5), O2–Li1–O4 96.1(5), O3–Li1–O4 103.7(5).

in the uranyl-bis(imidazolyl) complex **D** are 2.498(6) and 2.499(7) Å.<sup>[16]</sup> In contrast, the U–C bond length in  $[(\text{BIPMH})\text{UO}_2\text{Cl}(\text{THF})]$  (**A**) is much longer at 2.707(4) Å,<sup>[24]</sup> while the U–C bond length in the methanediide complex  $[\text{UO}_2(\text{SCS})(\text{py})_2]$  (**B**) is slightly shorter at 2.420(3) Å.<sup>[14]</sup> The longer U–C bond length in **1** compared to that calculated for the hexaalkyl  $[\text{U}(\text{CH}_2\text{SiMe}_3)_6]$  (**2**) complex (see Table 1) may be rationalized by the appreciable uranium–carbon antibonding character of the U–O  $\sigma$ -bonding molecular orbital (see HOMO-4 in Figure S10 in Supporting Information). The lithium cation in **1** exhibits a distorted tetrahedral geometry and is coordinated by one oxygen atom of the uranyl, two oxygen atoms of one DME ligand, and one oxygen atom from a DME ligand that bridges between two lithium cations. This bridging interaction results in the formation of a 1D polymer chain. The Li–O<sub>uranyl</sub> bond length (1.87(1) Å) is typical for lithium–oxo(uranyl) interactions.<sup>[23,25,26]</sup>

Our success in isolating and characterizing complex **1** prompted us to revisit the synthesis of  $[\text{U}(\text{CH}_2\text{SiMe}_3)_6]$  (**2**), which we initially reported in 2011.<sup>[5]</sup> Based on the recent theoretical study by Hrobárik et al., the  $^{13}\text{C}$  NMR chemical shift for the methylene carbon atoms of **2** is predicted to occur at an unprecedentedly high frequency when compared to other diamagnetic compounds.<sup>[19]</sup> This result contrasts greatly with our original assignment, which placed the resonance of the methylene moiety at 34.0 ppm in  $[\text{D}_8]\text{THF}$  at  $-40^\circ\text{C}$ .<sup>[5]</sup> However, it should be noted that the direct-detection  $^{13}\text{C}\{^1\text{H}\}$  NMR experiment was not performed with a large enough sweep width to observe a signal beyond 300 ppm.

Given the increasing interest in high-valent uranium–alkyl complexes, and considering that confirmation of the quantum-chemical prediction would greatly assist in the development of theoretical methods for the actinide elements, we re-recorded the  $^{13}\text{C}\{^1\text{H}\}$  NMR spectrum of **2** using a sufficiently large sweep width. Complex **2** was generated in  $[\text{D}_8]\text{THF}$  using the reported procedure,<sup>[5]</sup> and a  $^{13}\text{C}\{^1\text{H}\}$  NMR spectrum (from 0 to 1000 ppm) was recorded at  $-46^\circ\text{C}$ .

As was observed previously, the  $^{13}\text{C}\{^1\text{H}\}$  NMR spectrum of **2** exhibits a resonance at 11.2 ppm, which can be assigned to the methyl carbon atoms of the methyltrimethylsilyl ligand. More importantly, however, we also observed a resonance at 434.3 ppm, which we assigned to the methylene carbon atom of the  $\text{CH}_2\text{SiMe}_3$  ligand (Figure S7). This assignment was further confirmed in the HMBC spectrum (Figure S8). The chemical shift observed for the methylene carbon atom of **2** is the largest downfield shift yet observed for a diamagnetic compound containing a single metal atom.<sup>[29]</sup> Previously reported  $^{13}\text{C}$  NMR chemical shifts for carbon atoms directly bound to  $\text{U}^{\text{VI}}$  range from 262.8 ppm for  $[\text{UO}_2(\text{NHC}^{\text{C,N}})_2]$  ( $\text{NHC}^{\text{C,N}}$  = amido-tethered N-heterocyclic carbene),<sup>[26]</sup> to 329.4 ppm for  $[\text{Li}(\text{MeIm})][(\text{UO}_2(\text{Ar}_2\text{nacnac})(\text{C}_4\text{H}_5\text{N}_2)_2)]$  (**D**).<sup>[16]</sup> As shown in Ref. [19], these large high-frequency chemical shifts are, to an appreciable part, caused by relativistic spin–orbit (SO) coupling (see also  $\delta_{\text{SO}}$  in Table 1). An even more deshielded  $^{13}\text{C}$  NMR shift for **2** ( $\delta > 500$  ppm) is predicted when using 40% Hartree–Fock exchange in the density functional (PBE0-40HF). In this specific case, a reduction of exact-exchange admixture to 35% (PBE0-35HF) brings theory and experiment into better agreement, even more so upon shortening of the U–C bond by 0.01 Å when including dispersion corrections in the structure optimization (see Table S2 in Supporting Information). The effect of solvent included by a COSMO solvation model plays virtually no role for **2**, although its inclusion affects the computed shifts in **1** with more polarizable bonds (see Tables S1 and S2 in Supporting Information).

This unprecedented dependence on the functional for **2** is due to the extremely large SO contributions, which are influenced crucially by the core tails of the uranium valence 5f-orbitals. The choice of 40% exact exchange was motivated by a comparison to experimental data for only a handful of available  $^{13}\text{C}$  NMR shifts in complexes with direct  $\text{U}^{\text{VI}}$ –C  $\sigma$  bonds<sup>[19]</sup> (the use of PBE0-35HF for that series would actually worsen the agreement with experiment). In this respect, more experimental data for related uranium(VI) complexes are needed to improve and assess the computational methodology for the calculation of NMR shifts in organometallic uranium complexes to an accuracy that would be comparable to, for example, regular transition-metal complexes.

It is worth noting, that the  $^{13}\text{C}$  NMR resonances calculated for the methylene moieties of the analogous tungsten complexes  $[\text{W}(\text{CH}_3)_6]$  and  $[\text{W}(\text{CH}_2\text{SiMe}_3)_6]$  are 83.0 ppm and 98.8 ppm, respectively (Table 1). In these cases,  $\delta_{\text{SO}}$  contributes around 20 ppm to the total  $^{13}\text{C}$  NMR shift. This is more than one order of magnitude less than in the corresponding uranium(VI) complexes. The same holds for the comparison of the methylene  $^{13}\text{C}$  NMR resonances in complexes contain-

ing the  $\text{UO}_2^{2+}$  and  $\text{WO}_2^{2+}$  moieties (see Table 1). We note in passing, that  $\delta_{\text{SO}}$  in the title complexes **1** and **2** is almost as large as, or larger than, the entire range of  $^{13}\text{C}$  NMR chemical shifts in common organic compounds. A somewhat larger spin-orbit contribution ( $\delta_{\text{SO}} = 35.6$  ppm) than for the tungsten complexes can be noticed for the homoleptic pentaalkyl- $\text{Th}^{\text{IV}}$  complex. These tendencies clearly coincide with the role of 5f-orbitals in bonding, which is still relatively small for Th but large for U. The substantial high-frequency shift of the methylene carbon atom in **1** compared to that in the naked  $[\text{UO}_2(\text{CH}_2\text{SiMe}_3)_4]^{2-}$  anion is also largely caused by an increase of  $\delta_{\text{SO}}$ , again because of an increase of the f-orbital participation in bonding (see Table 1). These changes, and the excellent match of the experimentally observed  $^{13}\text{C}$  NMR chemical shifts of **1** with the computed ones, also support the coordination of solvated  $\text{Li}^+$  to the uranyl oxygen atoms in  $[\text{D}_8]\text{THF}$  solution. The extensive 5f participation in U–C bonding is also responsible for the octahedral structure of  $\text{U}^{\text{VI}}$ -hexaalkyl complexes. Optimizations of the formal  $5f^0$  complexes **1** and **2** without f functions in the basis set (the 4f shell is included in the pseudopotential core) result in prismatic structures similar to those of  $[\text{WMe}_6]$  and hypothetical  $[\text{W}(\text{CH}_2\text{SiMe}_3)_6]$ .<sup>[30,31]</sup>

To conclude, we have prepared and characterized the first genuine uranyl(VI)-alkyl complex  $[\text{Li}(\text{DME})_{1.5}]_2[\text{UO}_2(\text{CH}_2\text{SiMe}_3)_4]$  (**1**) by purposeful “ate” complex formation, and have confirmed its formulation by spectroscopic and X-ray crystallographic studies. The synthesis of the related homoleptic hexaalkyl complex  $[\text{U}(\text{CH}_2\text{SiMe}_3)_6]$  (**2**) and revision of its  $^{13}\text{C}$  NMR spectrum has allowed a meaningful comparison of the bonding situation in **1** and **2**, and analysis of the unprecedented high-frequency  $^{13}\text{C}$  NMR chemical shifts in these  $\text{U}^{\text{VI}}$  complexes. Computational analyses show that the 5f uranium character in U–C  $\sigma$  bond is larger in the hexaalkyl complex **2**, which is also reflected in the most deshielded  $^{13}\text{C}$  NMR shift observed in diamagnetic mononuclear compounds. Indeed, the comparison of computed and experimental  $^{13}\text{C}$  NMR data provides an important additional method for the analysis of covalent bonding and 5f-orbital participation in uranium(VI) complexes.

## Experimental Section

Synthesis of  $[\text{Li}(\text{DME})_{1.5}]_2[\text{UO}_2(\text{CH}_2\text{SiMe}_3)_4]$  (**1**). A cold ( $-25^\circ\text{C}$ ) solution of  $[\text{UO}_2\text{Cl}_2(\text{THF})_3]$  (74 mg, 0.13 mmol) in THF (2 mL) was added to a cold ( $-25^\circ\text{C}$ ) solution of  $\text{Li}(\text{CH}_2\text{SiMe}_3)$  (54 mg, 0.57 mmol) in DME (1 mL). This resulted in an immediate color change to deep red. The volatiles were removed in vacuo and the resulting red oil was triturated with hexanes (1 mL). The residue was then partially extracted into hexanes (4 mL) and the resulting green solution was filtered through a column of celite ( $2\text{ cm} \times 0.5\text{ cm}$ ) supported on glass wool. The volume of the filtrate was reduced in vacuo, and the solution was stored at  $-25^\circ\text{C}$  for 12 h, resulting in the deposition of green-yellow crystals (21.0 mg, 24% yield). Crystals of **1** suitable for analysis by X-ray crystallography were grown from a concentrated solution in hexanes stored at  $-25^\circ\text{C}$  for 16 h. Anal. Calcd for  $\text{C}_{28}\text{H}_{74}\text{Li}_2\text{O}_8\text{Si}_4\text{U}$ : C, 37.24; H, 8.26. Found (3 trials): C, 33.74; H, 7.28. C, 33.00; H, 6.77. C, 32.72; H, 7.33. Elemental analyses consistently showed low carbon and hydrogen content, likely because of the high thermal instability of **1**.  $^1\text{H}$  NMR (500 MHz,  $-1.6^\circ\text{C}$ ,  $[\text{D}_8]\text{THF}$ ):  $\delta = 3.43$  (br s, 12H,  $\text{CH}_2$  DME), 3.27 (br s, 18H,  $\text{CH}_3$

DME), 0.01 (s, 36H,  $\text{CH}_2\text{SiMe}_3$ ),  $-3.80$  ppm (s, 8H,  $\text{CH}_2\text{SiMe}_3$ ).  $^7\text{Li}\{^1\text{H}\}$  NMR (155 MHz,  $25^\circ\text{C}$ ,  $\text{C}_6\text{D}_6$ ):  $\delta = 2.93$  ppm (s).  $^{13}\text{C}\{^1\text{H}\}$  NMR (151 MHz,  $-1.6^\circ\text{C}$ ,  $[\text{D}_8]\text{THF}$ ):  $\delta = 242.9$  (s,  $\text{CH}_2\text{SiMe}_3$ ), 72.9 (s,  $\text{CH}_2$  DME), 59.1 (s,  $\text{CH}_3$  DME), 10.6 ppm (s,  $\text{CH}_2\text{SiMe}_3$ ). IR (KBr pellet):  $\tilde{\nu} = 1623$  (br, m), 1514 (sh), 1473 (sh), 1456 (w), 1417 (w), 1369 (w), 1290 (sh), 1246 (sh), 1211 (sh), 1196 (w), 1161 (sh), 1126 (w), 1111 (m), 1088 (m), 1072 (sh), 1034 (m), 972 (sh), 930 (br, m), 858 (s), 841 (s), 792 (sh), 758 (m), 698 (m), 671 (m), 615 (sh), 555 (sh),  $478\text{ cm}^{-1}$  (br, s).

NMR characterization of  $[\text{U}(\text{CH}_2\text{SiMe}_3)_6]$  (**2**). An NMR tube equipped with a J-Young valve was charged with a cold ( $-40^\circ\text{C}$ ) deep-green solution of  $[\text{Li}(\text{THF})_4][\text{U}(\text{CH}_2\text{SiMe}_3)_6]$  (30.1 mg, 0.028 mmol) in  $[\text{D}_8]\text{THF}$  (0.3 mL). A cold ( $-40^\circ\text{C}$ ) deep-red solution of  $[\text{U}(\text{OrBu})_6]$  (0.0211 mg, 0.031 mmol) in  $[\text{D}_8]\text{THF}$  (0.3 mL) was added to the first solution. Upon addition, the reaction mixture immediately turned deep gold in color. The NMR tube was then placed on dry ice and transported to an NMR spectrometer pre-cooled to  $-45.5^\circ\text{C}$ . Upon standing at  $-40^\circ\text{C}$ , a colorless, crystalline material formed, indicating the precipitation of  $[\text{Li}(\text{THF})_4][\text{U}(\text{OrBu})_6]$  from the reaction mixture.  $^1\text{H}$  NMR (500 MHz,  $-45.5^\circ\text{C}$ ,  $[\text{D}_8]\text{THF}$ ):  $\delta = 0.50$  (s, 54H,  $\text{CH}_2\text{SiMe}_3$ ),  $-3.16$  ppm (s, 12H,  $\text{CH}_2\text{SiMe}_3$ ).  $^{13}\text{C}\{^1\text{H}\}$  NMR (125 MHz,  $-45.5^\circ\text{C}$ ,  $[\text{D}_8]\text{THF}$ ):  $\delta = 434.3$  (s,  $\text{CH}_2\text{SiMe}_3$ ), 11.2 ppm (s,  $\text{CH}_2\text{SiMe}_3$ ).

Received: November 30, 2012

Published online: February 12, 2013

**Keywords:** actinides · bonding analysis · chemical shifts · spin-orbit coupling · uranyl compounds

- [1] H. Gilman, R. G. Jones, E. Bindshadler, D. Blume, G. Karmas, G. A. Martin, J. F. Nobis, J. R. Thirtle, H. L. Yale, F. A. Yoeman, *J. Am. Chem. Soc.* **1956**, 78, 2790–2792.
- [2] C. J. Burns, M. S. Eisen, *Organoactinide Chemistry: Synthesis and Characterization. In The Chemistry of the Actinide and Transactinide Elements*, Vol. 5 (Eds.: L. R. Morss, N. Edelstein, J. Fuger, J. J. Katz), Springer, Dordrecht, **2006**, pp. 2799–2910.
- [3] H. Gilman, *Adv. Organomet. Chem.* **1968**, 7, 33.
- [4] C. R. Graves, J. L. Kiplinger, *Chem. Commun.* **2009**, 3831–3853.
- [5] S. Fortier, J. R. Walensky, G. Wu, T. W. Hayton, *J. Am. Chem. Soc.* **2011**, 133, 11732–11743.
- [6] D. P. Mills, O. J. Cooper, F. Tuna, E. J. L. McInnes, E. S. Davies, J. McMaster, F. Moro, W. Lewis, A. J. Blake, S. T. Liddle, *J. Am. Chem. Soc.* **2012**, 134, 10047–10054.
- [7] For a recent review, see for example: R. J. Baker, *Chem. Eur. J.* **2012**, 18, 16258–16271.
- [8] a) W. Hallwachs, A. Schafarik, *Justus Liebigs Ann. Chem.* **1859**, 109, 206–209; b) J. Sand, F. Singer, *Justus Liebigs Ann. Chem.* **1903**, 329, 190–194.
- [9] M. J. Sarsfield, M. Helliwell, D. Collison, *Chem. Commun.* **2002**, 2264–2265.
- [10] See for example: a) J. P. Morizur, *Bull. Soc. Chim. Fr.* **1964**, 1331–1337; b) V. K. Grebenshchikov, V. N. Sokolov, G. M. Khvostik, G. P. Kondratenkov, *Khim. Urana (Dokl. Vses. Konf.)* **1981**, 292–296.
- [11] J.-C. Berthet, G. Siffredi, P. Thuery, M. Ephritikhine, *Dalton Trans.* **2009**, 3478–3494.
- [12] a) A. M. Seyam, *Inorg. Chim. Acta* **1982**, 58, 71–74; b) A. M. Seyam, *Inorg. Chim. Acta* **1985**, 110, 123–126.
- [13] M. J. Sarsfield, M. Helliwell, J. Raftery, *Inorg. Chem.* **2004**, 43, 3170–3179.
- [14] J.-C. Tourneux, J.-C. Berthet, T. Cantat, P. Thuery, N. Mezaillies, M. Ephritikhine, *J. Am. Chem. Soc.* **2011**, 133, 6162–6165.
- [15] J. Maynadie, J.-C. Berthet, P. Thuery, M. Ephritikhine, *Chem. Commun.* **2007**, 486–488.
- [16] M. F. Schettini, G. Wu, T. W. Hayton, *Chem. Commun.* **2012**, 48, 1484–1486.



- [17] S. Fortier, B. C. Melot, G. Wu, T. W. Hayton, *J. Am. Chem. Soc.* **2009**, *131*, 15512–15521.
- [18] L. A. Seaman, J. R. Walensky, G. Wu, T. W. Hayton, *Inorg. Chem.* **2013**, DOI: 10.1021/ic300867m.
- [19] P. Hrobárik, V. Hrobáriková, A. H. Greif, M. Kaupp, *Angew. Chem.* **2012**, *124*, 11042–11046; *Angew. Chem. Int. Ed.* **2012**, *51*, 10884–10888.
- [20] See also our recent study on unusually large spin–orbit effects on  $^1\text{H}$  NMR shifts in transition-metal–hydride complexes: P. Hrobárik, V. Hrobáriková, F. Meier, M. Repisky, S. Komorovsky, M. Kaupp, *J. Phys. Chem. A* **2011**, *115*, 5654–5659.
- [21] Crystal data for **1**:  $\text{C}_{28}\text{H}_{74}\text{Li}_2\text{O}_8\text{Si}_4\text{U}$ ,  $M_r = 903.14$ , space group  $P\bar{1}$ ,  $a = 10.5449(17)$ ,  $b = 11.530(2)$ ,  $c = 11.854(3)$  Å,  $\alpha = 101.773(5)$ ,  $\beta = 109.280(4)$ ,  $\gamma = 115.100(3)^\circ$ ,  $V = 1127.7(4)$  Å<sup>3</sup>,  $Z = 1$ ,  $\rho_{\text{calcd}} = 1.330$  g cm<sup>−3</sup>;  $\text{MoK}\alpha$  radiation,  $\lambda = 0.71073$  Å,  $\mu = 3.740$  mm<sup>−1</sup>,  $T = 100(2)$  K. 3568 measured reflections, 3520 unique reflections ( $R_{\text{int}} = 0.0852$ ),  $wR2 = 0.0984$ ,  $R_1 = 0.0411$ , GOF = 1.011. Residual electron density extrema were 2.03 and  $-2.38$  e Å<sup>−3</sup>.
- [22] L. R. Morss, N. M. Edelstein, J. Fuger, J. J. Katz, *The Chemistry of the Actinide and Transactinide Elements*, Springer, Dordrecht, **2006**.
- [23] S. Fortier, T. W. Hayton, *Coord. Chem. Rev.* **2010**, *254*, 197–214.
- [24] M. J. Sarsfield, H. Steele, M. Helliwell, S. J. Teat, *Dalton Trans.* **2003**, 3443–3449.
- [25] P. L. Arnold, I. J. Casely, Z. R. Turner, C. D. Carmichael, *Chem. Eur. J.* **2008**, *14*, 10415–10422.
- [26] S. A. Mungur, S. T. Liddle, C. Wilson, M. J. Sarsfield, P. L. Arnold, *Chem. Commun.* **2004**, 2738–2739.
- [27] P. Legzdins, E. C. Phillips, L. Sanchez, *Organometallics* **1989**, *8*, 940–949.
- [28] A. L. Galyer, G. Wilkinson, *J. Chem. Soc. Dalton Trans.* **1976**, 2235–2238.
- [29] To date, larger  $^{13}\text{C}$  NMR shifts (up to  $\delta = +486$  ppm) for diamagnetic compounds are known only for the interstitial carbon atom in some carbidocarbonyl–metal clusters, such as  $[\text{Fe}_5(\mu_5\text{-C})(\text{CO})_{15}]$  (see J. Mason, *J. Am. Chem. Soc.* **1991**, *113*, 6056–6062).
- [30] a) A. Haaland, A. Hammel, K. Rypdal, H. V. Volden, *J. Am. Chem. Soc.* **1990**, *112*, 4547–4549; b) V. Pfennig, K. Seppelt, *Science* **1996**, *271*, 626–628.
- [31] See also a detailed study on the role of f orbitals in structure preferences in hexafluoride and hydride complexes: M. Straka, P. Hrobárik, M. Kaupp, *J. Am. Chem. Soc.* **2005**, *127*, 2591–2599.